Observation of optical azimuthons

Alexander Minovich, Dragomir N. Neshev, Anton S. Desyatnikov, Wieslaw Krolikowski, and Yuri S. Kivshar

Nonlinear Physics Centre and Laser Physics Centre, Research School of Physics and Engineering, The Australian National University, Canberra, ACT 0200, Australia

dnn124@rsphysse.anu.edu.au

Abstract: We observe experimentally *optical azimuthons*, a generic class of ring-shaped localised spiralling beams with azimuthal modulation, carrying phase dislocation in self-focusing nonlinear media. We observe three- and four-lobe azimuthons in ^{87}Rb vapours and demonstrate their anomalous rotation controlled by the input phase distribution.

OCIS codes: (190.6135) Spatial solitons; (260.6042) Singular optics.

References and links

1. R. Y. Chiao, E. Garmire, and C. H. Townes, "Self-trapping of optical beams," Phys. Rev. Lett. **13**, 479 (1964).
2. Yu. S. Kivshar and G. P. Agrawal, *Optical Solitons: From Fibers to Photonic Crystals* (Academic, 2003).
3. A. S. Desyatnikov, Yu. S. Kivshar, and L. Torner, "Optical vortices and vortex solitons," Progress in Optics **47**, 291, Ed. E. Wolf (Elsevier, 2005).
4. V. I. Kruglov and R. A. Vlasov, "Spiral self-trapping propagation of optical beams in media with cubic nonlinearity," Phys. Lett. A **111**, 401 (1985).
5. C. Rotschild, O. Cohen, O. Manela, M. Segev, and T. Carmon, "Solitons in nonlinear media with an infinite range of nonlocality: first observation of coherent elliptic solitons and of vortex-ring solitons," Phys. Rev. Lett. **95**, 213904 (2005).
6. A. S. Desyatnikov and Yu. S. Kivshar, "Rotating optical soliton clusters," Phys. Rev. Lett. **88**, 053901 (2002).
7. A. S. Desyatnikov, A. A. Sukhorukov, and Yu. S. Kivshar, "Azimuthons: spatially modulated vortex solitons," Phys. Rev. Lett. **95**, 203904 (2005).
8. S. Lopez-Aguayo, A. S. Desyatnikov, Yu. S. Kivshar, S. Skupin, W. Krolikowski, and O. Bang, "Stable rotating dipole solitons in nonlocal optical media," Opt. Lett. **31**, 1100 (2006).
9. S. Lopez-Aguayo, A. S. Desyatnikov, and Yu. S. Kivshar, "Azimuthons in nonlocal nonlinear media," Opt. Express **14**, 7903 (2006); `http://www.opticsinfobase.org/abstract.cfm?URI=oe-14-17-7903`.
10. S. Skupin, M. Saffman, and W. Krolikowski, "Nonlocal stabilization of nonlinear beams in a self-focusing atomic vapor," Phys. Rev. Lett. **98**, 263902 (2007).
11. M. Soljacic and M. Segev, "Integer and fractional angular momentum borne on self-trapped necklace-ring beams," Phys. Rev. Lett. **86**, 420 (2001).
12. V. Tikhonenko, J. Christou, and B. Luther-Davies, "Spiraling bright spatial solitons formed by the breakup of an optical vortex in a saturable self-focusing medium," J. Opt. Soc. Am. B **12**, 2046 (1995).
13. M. S. Bigelow, P. Zerom, and R. W. Boyd, "Breakup of ring beams carrying orbital angular momentum in sodium vapor," Phys. Rev. Lett. **92**, 083902 (2004).
14. L. T. Vuong, T. D. Grow, A. Ishaaya, A. L. Gaeta, G. W. 't Hooft, E. R. Eliel, and G. Fibich, "Collapse of optical vortices," Phys. Rev. Lett. **96**, 133901 (2006).
15. G. A. Swartzlander, Jr. and C. T. Law, "Optical vortex solitons observed in Kerr nonlinear media," Phys. Rev. Lett. **69**, 2503 (1992).
16. S. M. Rochester, D. S. Hsiung, D. Budker, R. Y. Chiao, D. F. Kimball, and V. V. Yashchuk, "Self-rotation of resonant elliptically polarized light in collision-free rubidium vapor," Phys. Rev. A **63**, 043814 (2001).
17. N. N. Rozanov, "On the translational and rotational motion of nonlinear optical structures as a whole," Opt. Spectrosc. **96**, 405 (2004).

Self-trapping of light in two transverse dimensions [1,2] can lead to the formation of spatial optical solitons with complex power flow determined by phase singularities and spatial twist [3].

#119496 - $15.00 USD Received 4 Nov 2009; revised 7 Dec 2009; accepted 7 Dec 2009; published 9 Dec 2009

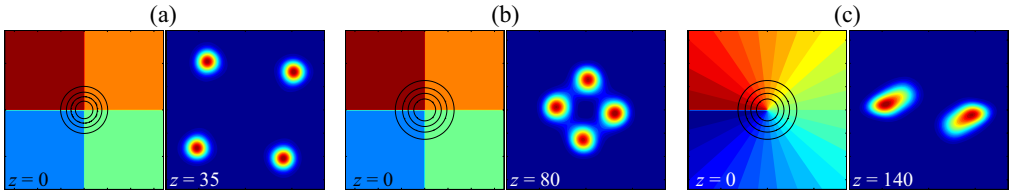

Fig. 1. Numerical results on phase imprinting: (a, Media 1) four-lobe unstable soliton cluster; (b, Media 2) four-lobe localised azimuthon formation; and (c, Media 3) unstable vortex soliton. Left: input phase profiles with superimposed intensity contours of the Gaussian beam. Right: intensity profiles after propagation distance indicated in the images.

Such solitons include the well known examples of vortex solitons [4,5] and soliton clusters [6]. The link between vortices and soliton clusters was recently revealed [7] through the existence of a generic family of spiralling solitons or *optical azimuthons*.

The azimuthon can be described as a vortex soliton continuously modulated along the ring with topological charge m and N-fold azimuthal modulation. Importantly, the azimuthon family (m,N) includes the known vortex soliton and the soliton cluster as particular members, with zero and maximum modulation depths, respectively. The presence of azimuthal intensity and phase modulation leads to spatial rotation of the ring, or spiralling, characterized by the angular velocity Ω. Remarkably, each family includes azimuthons with positive and negative Ω [7–10], so that spiralling is *anomalous* when the rotation is against the power circulation, determined by the topological charge m, e.g. $\Omega > 0$ for $m < 0$.

While the azimuthons represent a generic type of singular localized beams, they have never been observed experimentally in any physical system. Here, we report on the *first observation of optical azimuthons* employing rubidium vapours as an isotropic self-focusing nonlinear medium. The azimuthons are excited by a phase imprinting technique enabling the control of the input optical orbital angular momentum (OAM) by modifying intensity and phase profiles. We demonstrate that the nonlinear interaction of azimuthon lobes leads to slowing down of their spatial twist and inversion of the direction of rotation. We observe an anomalous spiralling for three-lobe azimuthons, rotating *opposite* to the overall power flow. This nonlinear wave phenomenon is in sharp contrast to the "mechanical" model of weakly interacting beams [11], which exhibit accelerated rotation for attracting lobes instead of the slowing down and inversion. Furthermore, when the initial phase lacks an azimuthal modulation, we observe a vortex breakup [12–14] instead of a robust rotation. This observation indicates that the presence of modulation stabilises the anomalously rotating azimuthons.

A theoretical approach unifying the complete family of optical azimuthons, including vortex solitons and soliton clusters, relies on the azimuthal "discretisation" of a vortex of charge m with imposed N-fold symmetry [7]. This discretisation can be described in terms of the series expansion of a vortex phase, $\theta(\varphi) = m\varphi$, near the azimuthal position, $\varphi_n = 2\pi n/N$, of the n-th intensity peak on the ring with radius R ($n = 1,..,N$):

$$\theta(\varphi) = m\varphi \simeq m\varphi_n + m(r/R)\sin(\varphi - \varphi_n) + \ldots, \qquad (1)$$

here (r,φ) are the polar coordinates in the transverse plane.

The *zero-order* term in Eq. (1) corresponds to a *soliton cluster* [6], i.e. a ring of N beams launched in parallel to each other with a staircase-like phase distribution. The *first-order* term [7] describes the additional azimuthal tilt of all lobes in the ring (initial twist). This tilt modifies the azimuthon OAM and provides generalization to the azimuthon family.

To illustrate the possibility for experimental excitation of optical azimuthons, we consider the lowest order azimuthon mode, with $m = 1$ and $N = 4$, radially stable in saturable media [6]. We test numerically the excitation of this mode by imposing four abrupt phase jumps on the input

#119496 - $15.00 USD Received 4 Nov 2009; revised 7 Dec 2009; accepted 7 Dec 2009; published 9 Dec 2009

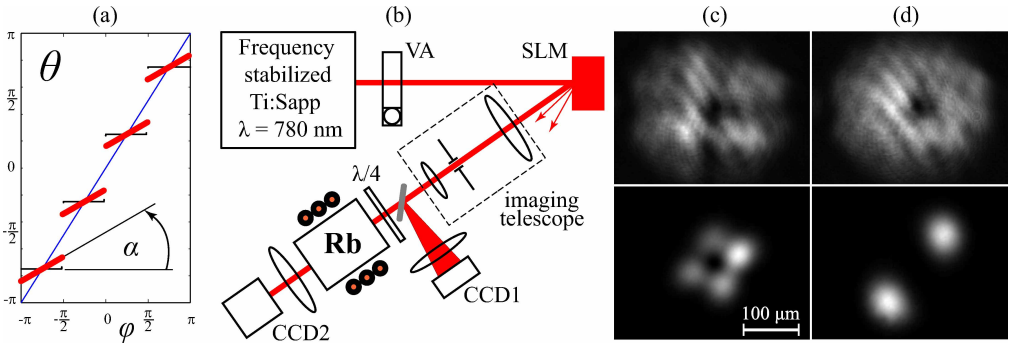

Fig. 2. (a) Phase distribution for generation of azimuthons. (b) Experimental setup: VA - variable attenuator, SLM - spatial light modulator, Rb - Rubidium cell, $\lambda/4$ - quarter wave-plate, CCD - cameras. (c, d) Experimental results: Input (top) and output (bottom) intensities for (c) an azimuthon with $\alpha = 0^\circ$ and (d) vortex with $\alpha = 45^\circ$. Input power 830 μW.

Gaussian beam [15], resulting also in an azimuthal intensity modulation. In Fig. 1 we present the evolution of the phase-imprinted Gaussian beam in a saturable nonlinear medium, $n_{\rm NL} = |E|^2/(1+|E|^2)$. The propagation distance given in the images is normalised to $z_0 = 1$ mm. We distinguish *three cases* of nonlinear beam propagation. In all cases, after initial reshaping, the beam acquires a vortex of charge $m = 1$ that is conserved with propagation. If the input power is lower than the power required for formation of an azimuthon-soliton-cluster we observe splitting of the beam into independent solitons [Fig. 1(a)]. The same step-like phase profile, however allows for mutual trapping of the four interacting lobes and formation of an azimuthon, if the power is increased [Fig. 1(b)]. For comparison, a vortex soliton with continuously twisted input phase [Fig. 1(c)] experiences azimuthal instability and breakup. The key result is the beam trapping in (b), suggesting that phase imprinting can be used to generate azimuthons.

To achieve excitation of the complete family of azimuthons, however, one has to implement the first-order contribution in Eq. (1). For this purpose, we introduce an additional parameter of azimuthal tilt α of the plane-sector phase segments [Fig. 2(a)], obtained by further expansion of Eq. (1) near $r \simeq R$ and $\varphi \simeq \varphi_n$:

$$\theta(\varphi) = m\varphi_n + m(\varphi - \varphi_n)\tan\alpha, \quad \text{for } |\varphi - \varphi_n| < \pi/N. \tag{2}$$

Here $\alpha = 0$ corresponds to the zero-order soliton cluster, while for $\alpha > 0$ or $\alpha < 0$ we have phase of each lobe tilted alongside or opposite the direction of the vortex phase twist. The vortex phase is recovered at $\alpha = \pi/4$. We also choose $\varphi_n = \pi(2n-1)/N - \pi$ to map this phase to the domain $\theta \in m(-\pi, \pi)$.

To prove experimentally the existence of optical azimuthons, we employ the experimental setup shown in Fig. 2(b). We use a frequency stabilised cw Ti:Sapphire laser (linewidth of < 10 MHz at 780 nm), detuned by 0.66 GHz to the blue-side of the ^{87}Rb resonance $5S_{1/2}F = 1 \rightarrow 5P_{3/2}F = 0,1,2$ (~ 1 GHz spectral width) [16]. The Gaussian laser beam is expanded and directed at a small angle to a reflective spatial light modulator (SLM). The SLM imprints a holographic grating that is truncated at the required beam width and thus allows for precise phase and coarse intensity modulation in the first diffraction order [selected by the iris diaphragm in the imaging telescope in Fig 2(b)]. The spatially modulated beam is subsequently imaged onto the input window of a 8 cm long Rb cell (at 166°C) by a telescope with sixteen times demagnification. Strong magnetic field is applied along the cell to avoid the influence of Earth's magnetic field on the Zeeman splitting of energy levels. The input and output intensity distributions of the circularly polarized light are recorded simultaneously onto two CCD cameras.

First we study the four-lobe soliton cluster from the azimuthon family at $\alpha = 0$, as in

#119496 - $15.00 USD Received 4 Nov 2009; revised 7 Dec 2009; accepted 7 Dec 2009; published 9 Dec 2009

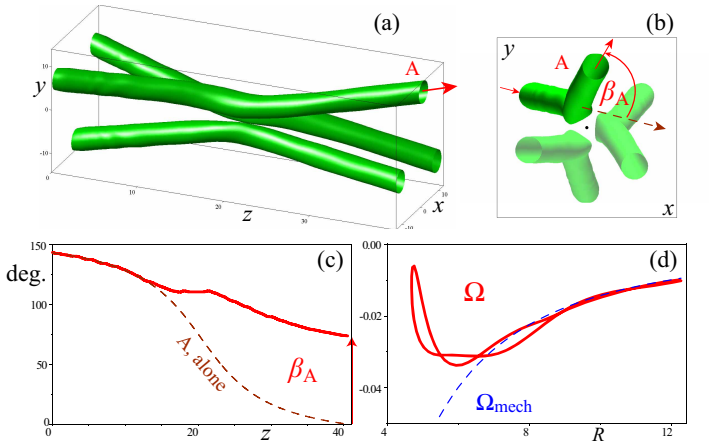

Fig. 3. Calculated dynamics of three beams in saturable media (Media 4). (a) 3D and (b) transverse views of the interacting beams showing their twist due to interaction. The twist is characterized by the angle β_A (c) and by the angular velocity Ω (d).

Figs. 1(a), 1(b). We vary the beam power and waist at a fixed detuning and Rb cell temperature and for the input intensity profile shown in Fig. 2(c-top) we observe a strongly localized four-peak structure [Fig. 2(c-bottom)] at the cell output (corresponding to approximately 2.5 diffraction lengths of propagation). This result agrees well with the initial numerical simulations shown in Fig. 1(b). Furthermore, we test the generation of the four-lobe azimuthons in a series of measurements modifying the phase profile (2) with different $\alpha > 0$. We observe rotation of the output intensity profile, however, the four-peak azimuthon structure appears highly unstable and transforms into two independent solitons already for $\alpha \gtrsim 10^\circ$. This behaviour is similar to the break-up of a vortex soliton, shown in Fig. 2(d).

The results for the four-lobe azimuthons above suggest that they can be approximately described as a ring of N fundamental solitons tilted in azimuthal direction. The total field, $E = \sum_{n=1}^{N} G_n$, governed by paraxial nonlinear Shrödinger (NLS) equation, $2ik\partial_z E + \Delta E + n\left(|E|^2\right)E = 0$, is taken at $z = 0$ as a superposition of Gaussian beams,

$$G_n = A\exp\left(-|\mathbf{r}-\mathbf{r}_n|^2/2w^2 + im\varphi_n + ik\mathbf{v}_n(\mathbf{r}-\mathbf{r}_n)\right), \tag{3}$$

where $\mathbf{r}_n = R\{\cos\varphi_n, \sin\varphi_n\}$, the initial transverse velocity $\mathbf{v}_n = \tan\gamma\{-\sin\varphi_n, \cos\varphi_n\}$, and γ is the tilt angle of each beam with respect to the optical axis z. The vortex phase (1) is recovered in Eq. (3) for $\tan\gamma = m/kR$. This value for the initial twist results in the formation of an unstable vortex soliton [6].

To show that the ansatz Eq. (3) can serve as a rough approximation for the azimuthon [7–10] we simulate the propagation in saturable media of three beams placed far from each other so that their interaction at the input can be neglected, see Fig. 3. The initial tilts are arranged such that the beams rotate clockwise and collide. The beam phases are also twisted clockwise, i.e. the vortex charge $m = -1$ in Eq. (3). The noninteracting beams propagate along straight lines, see dashed arrow in Fig. 3(b) for the beam A. The interaction of the beams, however, strongly alters their paths. This is clearly visible in Fig. 3(c), where the transverse angle β_A is measured from the characteristic $\tan^{-1}$ curve for a straight beam (marked "A, alone"). Importantly, the beam twist is *counter-clockwise*, against the transverse energy flow.

This observation directly demonstrates the essence of the nontrivial rotation of azimuthons. The angular velocity Ω, calculated during propagation [17] is shown in Fig. 3(d) versus radius of azimuthon, $R^2 = \int |E|^2\mathbf{r}^2 d\mathbf{r}$. For comparison, we also show with a dashed line

#119496 - $15.00 USD Received 4 Nov 2009; revised 7 Dec 2009; accepted 7 Dec 2009; published 9 Dec 2009

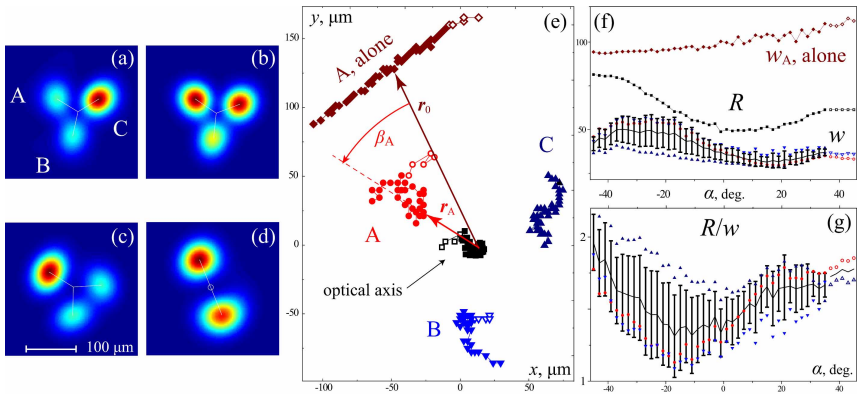

Fig. 4. Three lobe azimuthon experiments. (a-d) Measured output profiles for input tilts $\alpha = 1^\circ, 15^\circ, 29^\circ, 43^\circ$ and power $690\,\mu$W. (e) Output positions of the three lobes compared with the position of a single noninteracting lobe, marked "A, alone". The azimuthon radius R and the average width of each beam w are shown in (f) and their ratio in (g).

the "mechanical" rotation velocity, $\Omega_{\rm mech} = 2M/PR^2$. Here the beam angular momentum is $M = {\rm Im}\int E^* E_\varphi d\mathbf{r}$ and its power is $P = \int |E|^2 d\mathbf{r}$. The conservation of M, in the mechanical picture, leads to the "skater on ice" effect [11], when the absolute value of $\Omega_{\rm mech}$ increases for smaller radius R. This is not the case for azimuthons: in the region of strong interaction of the beams (small R), the angular velocity Ω decreases and the rotation slows down.

To test these predictions, in our experiments we apply a three-sector phase imprinting to generate a three-lobe azimuthon with strongly localised and bound lobes at input power of $690\,\mu$W (Fig. 4). We then perform a series of measurements varying input phase α from -45° to 45°, with a step of 2°. As we increase α, we observe the rotation of all three peaks at the output [Figs. 4(a)–4(c)]. This rotation is followed by a sudden transformation into two independent solitons [Fig. 4(d)] when phase pattern approaches continuous vortex distribution ($\alpha \gtrsim 36^\circ$). Please note that in Figs. 4(a), 4(c) the lobes of the azimuthons appear asymmetric as a consequence of imperfect initial excitation. In Fig. 4(e) we plot the transverse coordinates of the three beams [marked A, B, and C in (a)] at the output of the Rb cell together with coordinates of a beam "A, alone" propagating along a straight line. Position of the optical axis is determined at the centre of a circle passing through the three beams. The fluctuation of its location shows the level of error in our measurements. The ring radius R is plotted in (f), together with the averaged width w of each lobe, approximated by a Gaussian. Note that: (i) the three beams are strongly attracted [cf. positions of beams A and "A, alone" in (e)], and (ii) azimuthon lobes are focused stronger than the same beam propagating alone [see curve in (f) marked "w_A, alone"]. As a result, the ratio R/w [Fig. 4(g)] remains in the limits $1 \leq R/w \leq 2$, indicating strong overlap and interaction between azimuthon lobes.

The experimentally measured angle of azimuthon rotation β is plotted in Fig. 5(a) versus the input angle α. In a good qualitative agreement with the numerical results [Fig. 3(c), $\beta_A > 0$], the experimentally measured output angle β is *always positive* in Fig. 5(a). This means that the azimuthon rotates counter-clockwise, i.e. *against its power circulation* determined by the vortex phase with $m = -1$. Thus we observe the *anomalous spiralling* of mutually trapped lobes through the *formation of an azimuthon*.

It is important to note that the relation between the experimentally controlled input (angular momentum M) and the measured output (angular position β) lies in the dynamics of angular velocity Ω. In contrast to numerics, however, Ω is not directly measurable in experiment. In particular, while in Fig. 3 the dynamics is shown during propagation along z and for a given

#119496 - $15.00 USD Received 4 Nov 2009; revised 7 Dec 2009; accepted 7 Dec 2009; published 9 Dec 2009

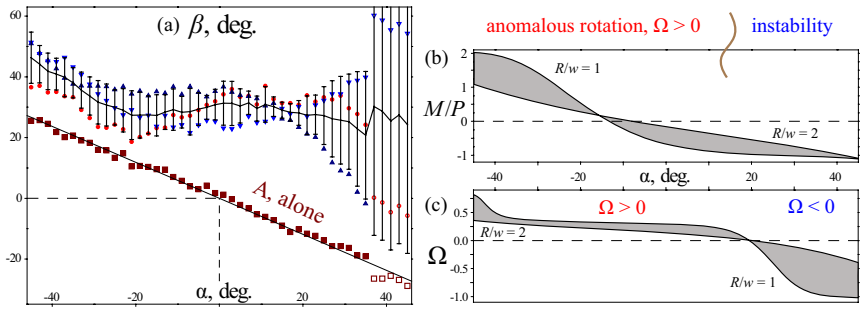

Fig. 5. Anomalous spiralling: (a) markers show the output angles measured for each beam such as β_A in Fig. 4(e), the error bars indicate standard deviation from the mean value β (solid line). Numerically calculated OAM (b) and angular velocity (c) for the three-lobe azimuthon Eq. (3) in saturable media; shaded is the domain $1 \le R/w \le 2$.

value of the input angular momentum M (integral of motion), in experiments we measure the angle β at the output ($z = L$) for a varying input angular momentum, $M = M(\alpha)$.

To clarify the relation between propagation dynamics in Fig. 3 and the output parametrization in Fig. 5(a), we use the ansatz Eq. (3) and calculate the ratio M/P versus α [Fig. 5(b)] with $N = 3$ and $m = -1$ in the domain $1 \le R/w \le 2$, similar to experiments. The OAM varies significantly with α: note that for $\alpha \lesssim -15^\circ$ the OAM is positive despite the fact that the topological charge is negative; for $\alpha \to 45^\circ$ it approaches the value $M/P = m = -1$ of the vortex soliton. The OAM alone, however, does not define the rotation velocity Ω and the output angle β, as seen from comparison between Figs. 5(a, b). The velocity Ω is determined by the nonlinear propagation [17] (parameters of the medium) and the absorption in the Rb vapors may have a strong effect. Also, we expect a breathing dynamics of self-trapping and non-uniform azimuthon rotation, $\Omega = \Omega(z)$, inside the medium. Thus the output angle, $\beta = \int_0^L \Omega(z)dz$, can not be estimated simply as $L\Omega$, where L is the length of Rb cell. Nevertheless, we calculate Ω [see Fig. 5(c)] for the ansatz (3) in saturable medium [17] and find remarkable qualitative agreement with the experimental results in Fig. 5(a).

We distinguish two major regions of interest in Fig. 5. The first domain of $\alpha \lesssim 20^\circ$ is approximately marked "anomalous rotation" in (b) because it corresponds to counter-clockwise twist with positive angle $\beta > 0$ in (a) and positive angular velocity $\Omega > 0$ in (c). In the second domain, $\alpha \gtrsim 20^\circ$, the rotation is expected to be normal, $\Omega < 0$, in accordance with Fig. 5(c). In experiment, however, the errors grow noticeably in Fig. 5(a) because we observe an onset of azimuthal instability. Indeed, for $\alpha \gtrsim 36^\circ$, approaching the vortex phase at $\alpha = 45^\circ$, we observe two beams at the output [Fig. 5(d)] instead of the three-lobe azimuthon, a typical output of the breakup of a vortex soliton [12]. Therefore, we mark this domain as "instability" in Fig. 5(b).

Our observations of the three-lobe azimuthon can be summarized as follows. First, the three-fold phase pattern at the input generates an azimuthon with three lobes mutually trapped and strongly interacting [Fig. 4]. Second, by changing the input tilt angle α and the OAM in experiment we observe the anomalous rotation of the three-lobe azimuthon [Figs. 5(a), 5(c)]. Finally, the comparison of Figs. 4(a)–4(c) against Fig. 4(d) and the analysis of Fig. 5, demonstrate the stabilizing effect of anomalous rotation on the dynamics of azimuthons.

In conclusion, we have generated experimentally optical azimuthons as a generic class of self-trapped spiralling beams in nonlinear media. Our results suggest that the modulation of the power flow along the azimuthal coordinate leads to the slowing down of azimuthon rotation and provides an effective mechanism for their stabilization in comparison to the unstable vortex solitons. We believe that these results provide further insight into fundamental properties of optical angular momentum and twisted light in nonlinear media.

#119496 - $15.00 USD Received 4 Nov 2009; revised 7 Dec 2009; accepted 7 Dec 2009; published 9 Dec 2009

Acknowledgements

We acknowledge help by M. Saffman and support from the Australian Research Council.

#119496 - $15.00 USD Received 4 Nov 2009; revised 7 Dec 2009; accepted 7 Dec 2009; published 9 Dec 2009